



Cite this: *Chem. Commun.*, 2015, 51, 11860

Received 6th June 2015,  
Accepted 19th June 2015

DOI: 10.1039/c5cc04675k

www.rsc.org/chemcomm

# A Cu<sub>4</sub>S model for the nitrous oxide reductase active sites supported only by nitrogen ligands†

Brittany J. Johnson,<sup>a</sup> William E. Antholine,<sup>b</sup> Sergey V. Lindeman<sup>c</sup> and Neal P. Mankad<sup>\*a</sup>

To model the (His)<sub>7</sub>Cu<sub>4</sub>S<sub>n</sub> (*n* = 1 or 2) active sites of nitrous oxide reductase, the first Cu<sub>4</sub>(μ<sub>4</sub>-S) cluster supported only by nitrogen donors has been prepared using amidinate supporting ligands. Structural, magnetic, spectroscopic, and computational characterization is reported. Electrochemical data indicates that the 2-hole model complex can be reduced reversibly to the 1-hole state and irreversibly to the fully reduced state.

Nitrous oxide reductase (N<sub>2</sub>OR) is a copper-dependent enzyme that converts environmentally harmful nitrous oxide into benign dinitrogen and water during bacterial denitrification.<sup>1</sup> Two forms of the N<sub>2</sub>O-reducing active site of N<sub>2</sub>OR have been characterized crystallographically (Fig. 1a). Both feature Cu<sub>4</sub>(μ<sub>4</sub>-S) cores supported by seven histidine N-donors; the Cu<sub>Z</sub><sup>\*</sup> form features a hydroxide/water ligand along one edge of the tetra-copper cluster,<sup>2,3</sup> while the Cu<sub>Z</sub> form instead features a second sulphide ligand along that edge.<sup>4</sup> The Cu<sub>Z</sub><sup>\*</sup> site has a “1-hole” Cu<sup>I</sup><sub>3</sub>Cu<sup>II</sup> resting state and activates N<sub>2</sub>O rapidly in the “fully reduced” Cu<sup>I</sup><sub>4</sub> state, while the Cu<sub>Z</sub> site has a “2-hole” Cu<sup>I</sup><sub>2</sub>Cu<sup>II</sup><sub>2</sub> resting state and activates N<sub>2</sub>O slowly in its “1-hole” state.<sup>5</sup> The electronic structure descriptions and chemical mechanisms related to these active sites remain elusive, motivating model studies.

Much of the available knowledge regarding copper sulphide clusters comes from studies of Cu<sub>2</sub>S<sub>2</sub><sup>6</sup> and Cu<sub>3</sub>S<sub>2</sub><sup>7,8</sup> model complexes, which feature bridging ligands with significant S–S interactions,<sup>9</sup> supported by nitrogen chelates. The latter category of complexes (Fig. 1b), in particular, has been the subject of extensive experimental and computational characterization as well as fascinating literature discussions.<sup>9–11</sup>

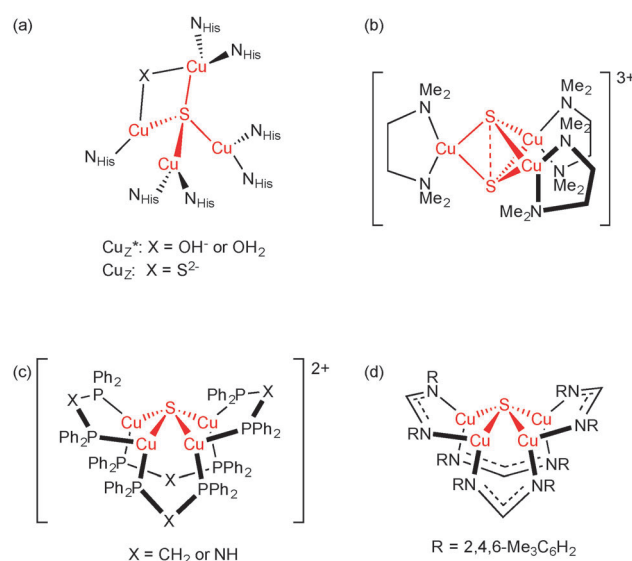


Fig. 1 (a) Structures of the Cu<sub>Z</sub><sup>\*</sup> and Cu<sub>Z</sub> active sites of nitrous oxide reductase; (b) a representative Cu<sub>3</sub>S<sub>2</sub> model complex with nitrogen ligands; (c) previously reported Cu<sub>4</sub>(μ<sub>4</sub>-S) model complexes with phosphorous ligands; (d) the Cu<sub>4</sub>(μ<sub>4</sub>-S) model complex reported in this work.

However, none of these complexes truly model the unusual μ<sub>4</sub>-S bridge of N<sub>2</sub>OR or provide insight into reduced catalytic intermediates. Phosphine<sup>12,13</sup> ligands have been used to stabilize “fully reduced” Cu<sub>4</sub>(μ<sub>4</sub>-S) and Cu<sub>3</sub>(μ<sub>3</sub>-S) clusters more structurally faithful to N<sub>2</sub>OR (Fig. 1c), but the inability thus far of these systems to access open-shell oxidation states has precluded experimental determination of electron structure using typical methods of physical inorganic chemistry.<sup>14</sup> In this regard, a recent report of strained Cu<sub>3</sub>(μ<sub>3</sub>-S) clusters encapsulated within a tris-(β-diketiminate) cyclophane cage was a noteworthy advance.<sup>15</sup> In this communication, we report the first Cu<sub>4</sub>(μ<sub>4</sub>-S) cluster supported only by nitrogen ligands (Fig. 1d) and disclose its structural, magnetic, and spectroscopic characterization. This system will provide an entry point for electronic structure determination and chemical reactivity studies for a tetracopper

<sup>a</sup> Department of Chemistry, University of Illinois at Chicago, Chicago, IL, USA.  
E-mail: npm@uic.edu

<sup>b</sup> Department of Biophysics, Medical College of Wisconsin, Milwaukee, WI, USA

<sup>c</sup> Department of Chemistry, Marquette University, Milwaukee, WI, USA

† Electronic supplementary information (ESI) available: Experimental and computational methods, spectral and crystallographic data, computational output. CCDC 1405092 (1). For ESI and crystallographic data in CIF or other electronic format see DOI: 10.1039/c5cc04675k

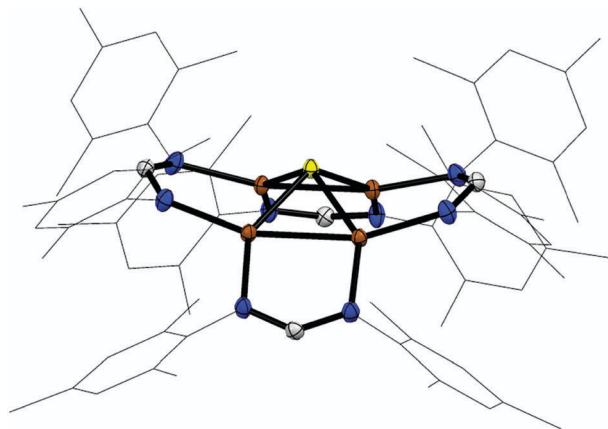


Fig. 2 X-ray structure of **1**, with only one of two disordered  $\text{Cu}_4\text{S}$  components shown. Mesityl groups are shown as wireframes, other atoms are shown as 50%-probability thermal ellipsoids, and hydrogen atoms have been omitted. Colour scheme: C, grey; Cu, brown; N, blue; S, yellow.

sulphide environment that is, arguably, the most relevant model for  $\text{N}_2\text{OR}$  identified to date.

Inspired by a recent study of copper amidinate clusters assembled using carbon disulphide,<sup>16</sup> we sought to study copper sulphide chemistry using the amidinate ligand,  $[(2,4,6\text{-Me}_3\text{C}_6\text{H}_2\text{N})_2\text{CH}]^-$  (abbreviated  $\text{NCN}^-$  here). Addition of the neutral sulphur atom donors  $\text{S}_8$  or  $\text{Ph}_3\text{SbS}$  to the dicopper(i) precursor  $(\text{NCN})_2\text{Cu}_2$  resulted in a dramatic colour change from colourless to dark purple. While this purple product (**1**) formed in low yields due to its instability in solution as well as the formation of several side products, we were able to isolate **1** in yields of 34–43%. Elemental analysis data for this material was consistent with a  $(\text{NCN})_4\text{Cu}_4\text{S}$  stoichiometry, and this assignment was confirmed by single-crystal X-ray diffraction. Complex **1** crystallizes in the  $P4_3n$  space group. The crystal symmetry coincides with the local symmetry of the  $\text{NCN}^-$  ligand shell, which is highly ordered about the crystallographic  $\bar{4}$  axis through possible stabilization from  $\pi$ -stacking interactions (Fig. 2). (This structure is apparently rigid in solution as evidenced by NMR spectroscopy, where six distinct mesityl methyl resonances were resolved, indicating restricted  $\text{N-C}_{\text{aryl}}$  bond rotation as well as static pseudo- $\text{S}_4$  symmetry in solution that distinguishes the “upwards”  $\text{NCN}^-$  ligands from the “downwards”  $\text{NCN}^-$  ligands. See Fig. S5, S6 and S16, ESI†). However, the crystal symmetry results in two alternative positions for the  $\text{Cu}_4\text{S}$  core that apparently has lower internal symmetry (Fig. S15, ESI†).

The exact assignment of alternative Cu and S positions to one or another component of the crystallographic disorder was done by analysing Cu–Cu and Cu–S separations from the point of view of structurally meaningful values. This assignment was confirmed by DFT calculations. Spin-unrestricted and symmetry-unrestricted DFT calculations at the BVP86/LANL2TZ(f) level of theory were conducted for both singlet and triplet spin states using a model where the *N*-mesityl groups were changed to *N*-methyl groups (**1-Me**). The singlet state for **1-Me** was calculated to be lower in energy than the triplet state (by  $10.2 \text{ kcal mol}^{-1}$ , although more advanced calculations would be needed to

accurately estimate the singlet–triplet gap). The optimized structure of the singlet state has  $\text{C}_{2v}$  symmetry and is characterized by an alternating short–long–short–long pattern of Cu–Cu distances within the  $\text{Cu}_4$  rectangle, with short Cu–Cu distances of  $2.45 \text{ \AA}$  and long Cu–Cu distances of  $2.79 \text{ \AA}$ . It is tempting, based on these bond distances, to view the **1-Me** structure as consisting of two separate  $[\text{Cu}^{1.5}\text{Cu}^{1.5}]$  units that are antiferromagnetically coupled to each other, giving rise to the singlet ground state. However, the two optimized structures were found to have stable wavefunctions with respect to internal magnetic coupling, and the  $\alpha$  and  $\beta$  molecular orbitals for the singlet state were degenerate and identical in nature. Collectively, these observations indicate that **1-Me** is best described at this time as having a closed-shell singlet ground state rather than a singlet state arising from magnetic coupling, at this level of theory.

Only one  $\text{Cu}_4\text{S}$  set can be identified from the disordered crystal structure of **1** that matches the topology and key structural features of optimized singlet **1-Me**. The resulting structure (Fig. 2) for **1** possesses near-perfect  $\text{C}_{2v}$  symmetry and replicates the calculated bond length alternation in the  $\text{Cu}_4$  rectangle of **1-Me**, with experimentally determined short Cu–Cu distances of  $2.4226(6) \text{ \AA}$  and long Cu–Cu distances of  $3.0353(6) \text{ \AA}$ . Within this component, the two sets of Cu–S distances are  $2.1812(6) \text{ \AA}$  and  $2.1790(6) \text{ \AA}$ . The geometry at sulphur is characterized by a  $\tau_4$  value<sup>17</sup> of 0.76, similar to the  $\tau_4$  values for the  $\mu_4\text{-S}$  ligands in  $\text{Cu}_Z^*$  (0.66) and  $\text{Cu}_Z$  (0.71).

The formal oxidation state assignment for **1** is  $\text{Cu}_2^{\text{I}}\text{Cu}_2^{\text{II}}$ , making it a model for the “2-hole” state of the  $\text{N}_2\text{OR}$  active site. The 2-hole  $\text{Cu}_Z$  is also a singlet ground state.<sup>1</sup> The purple colour of **1** comes from two overlapping absorbance peaks (Fig. 3): a main peak centred at  $561 \text{ nm}$  ( $\epsilon \approx 14\,000 \text{ M}^{-1} \text{ cm}^{-1}$ ) and a shoulder at approximately  $470 \text{ nm}$ . For comparison, the 2-hole  $\text{Cu}_Z$  absorbs at  $540 \text{ nm}$  and the 1-hole  $\text{Cu}_Z^*$  absorbs at  $680 \text{ nm}$ .<sup>5</sup> To our knowledge, the 2-hole  $\text{Cu}_Z^*$  has not been characterized.

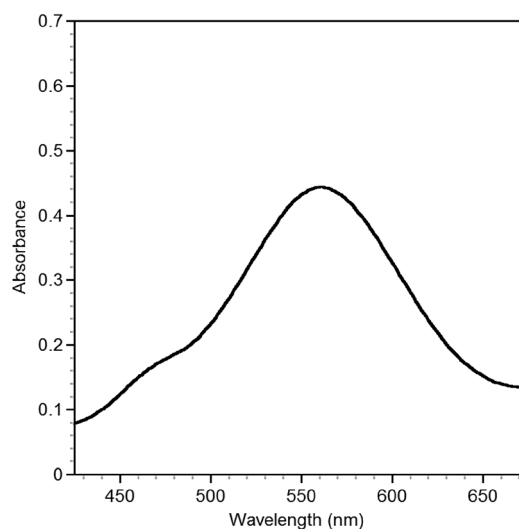


Fig. 3 Absorbance spectrum of **1** (0.06 mM solution in  $\text{CH}_2\text{Cl}_2$ ).

The accumulated experimental data is consistent with **1** possessing a singlet ground state with a low-energy triplet excited state. The  $^1\text{H}$  and  $^{13}\text{C}\{^1\text{H}\}$  NMR spectra for **1** resemble those for a typical diamagnetic species, with chemical shifts occurring in their normal regions. However, complex **1** exhibits a measurable magnetic moment in solution that increases with increasing temperature ( $\mu_{\text{eff}} = 2.3\text{--}2.9 \mu_{\text{B}}$  over the temperature range 221–298 K; see Fig. S1, ESI†). In addition, a frozen glass containing **1** was found to be EPR active. The observed EPR spectrum seems typical for a monomeric  $S = 1/2$  cupric species with splitting from one Cu and two equivalent N centres ( $g_{\parallel} = 2.134$ ,  $A_{\parallel}(\text{Cu}) = 185 \text{ G}$ ,  $A_{\parallel}(\text{N}) = 15 \text{ G}$ ; see Fig. S18a and b, ESI†). Notably, the intensity of the EPR signal was found to increase by a factor of 2.5 as the temperature was increased from 115 K to 130 K. Upon decreasing the temperature from 130 K to 112 K, the signal intensity decreased, indicating that the temperature dependence is reversible. For a typical  $S = 1/2$  signal, the Curie Law predicts that

the signal intensity should decrease by a factor of  $115/130 = 0.88$  when warmed from 115 K to 130 K, as we confirmed by analysing  $\text{Cu}(\text{acac})_2$  as an authentic  $S = 1/2$  control sample (Fig. S18c, ESI†). The increase in signal intensity with increasing temperature could be a further indication that a paramagnetic excited state is being thermally populated. While it is not clear how the observed EPR signal fits the magnetic properties of **1**, the reversible temperature dependence is unusual. Even if after further studies the  $S = 1/2$  signal turns out to derive from a trace paramagnetic byproduct or decomposition material, or even from a temperature-dependent comproportionation equilibrium, the magnetic properties for the EPR-active complex are novel and warrant further explanation, which is beyond the scope of this investigation. It is worth noting that there is precedent for dicopper sites with EPR spectra resembling monomeric cupric species.<sup>18–21</sup>

The cyclic voltammetry of **1** was examined in both  $\text{CH}_2\text{Cl}_2$ , which provides access to more oxidizing potentials, and THF, which provides access to more reducing potentials. In  $\text{CH}_2\text{Cl}_2$  (Fig. 4a), the cyclic voltammogram (CV) of **1** featured a reversible wave centred at  $-1.28 \text{ V vs. Fc}^+/\text{Fc}$  ( $\text{Fc}$  = ferrocene), which is assigned as the  $1/[1]^-$  couple, as well as two quasi-reversible waves at  $+0.51$  and approximately  $+0.92 \text{ V vs. Fc}^+/\text{Fc}$ . These oxidative events are assigned as ligand-based oxidations for two reasons. First, nearly identical signatures were found in the CV of the  $(\text{NCN})_2\text{Cu}_2$  precursor (Fig. S11, ESI†). Second, a closely related amidinate-supported dicopper system is known to engage in predominantly ligand-based redox chemistry at

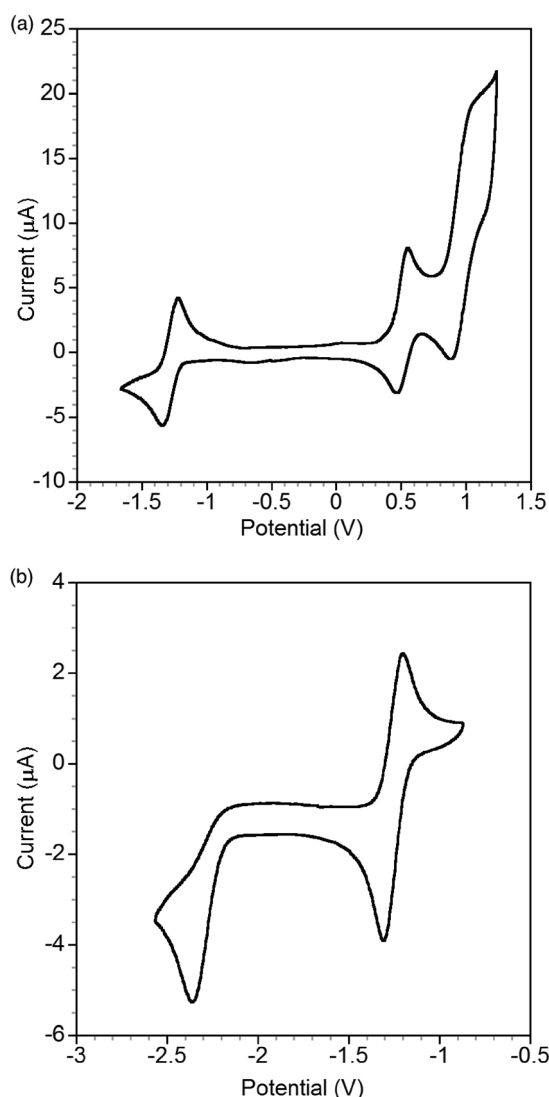


Fig. 4 Cyclic voltammograms of **1** with 0.1 M  $[\text{NBu}_4][\text{PF}_6]$  electrolyte in (a)  $\text{CH}_2\text{Cl}_2$  and (b) THF.

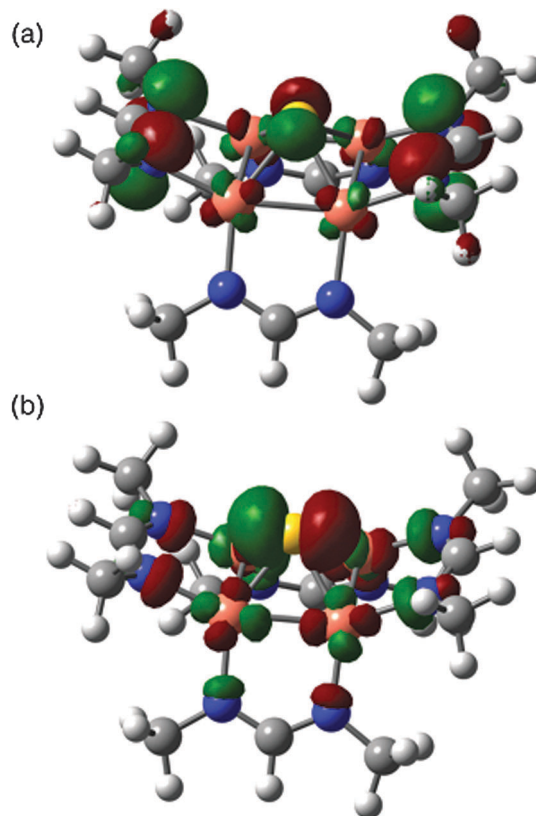


Fig. 5 Calculated (a) HOMO and (b) LUMO for **1-Me** (0.04 isovalue).

similar potentials.<sup>22</sup> In THF (Fig. 4b), the  $1/[1]^-$  couple was observed at  $-1.25$  V vs.  $Fc^+/Fc$ , and an additional irreversible reduction to  $[1]^{2-}$  was observed with onset at approximately  $-2.36$  V vs.  $Fc^+/Fc$ . Collectively, the CV data indicates that (a) oxidation of **1** occurs from the  $NCN^-$  ligands, (b) the formally  $Cu^I_3Cu^{II}$  “1-hole” species also is stabilized in this system, and (c) further ligand modification is needed to stabilize the formally  $Cu^I_4$  “fully reduced” oxidation state that would model the active form of  $Cu_Z^*$ .

Lastly, information about the frontier orbitals can be obtained from the calculated DFT structure of **1-Me** and is largely consistent with the collected experimental data. The calculated **1-Me** HOMO (Fig. 5a), which models the source of electrons during oxidation of **1**, is mostly based on two of the  $NCN^-$  ligands, with MO populations of 60% total N 2p (15% each), 7% S 3p, and 16% total Cu 3d (4% each). The calculated **1-Me** LUMO (Fig. 5b), which models the destination of electrons during reduction of **1** to the 1-hole and fully reduced states, is mostly based on the covalent  $Cu_4(\mu_4S)$  core, with MO populations of 21% S 3p, 48% total Cu 3d (12% each), and 12% total N 2p (3% each).

In conclusion, this report discloses the synthesis and thorough characterization of copper sulphide cluster **1**, which represents the most relevant model for the active sites of  $N_2OR$  to date from the perspective of featuring a  $Cu_4(\mu_4S)$  core supported only by nitrogen ligands. While structurally similar to the  $Cu_Z^*$  site, model **1** possesses redox chemistry reminiscent of the more electron-rich  $Cu_Z$  site, presumably due to the presence of anionic amidinate ligands in place of neutral histidine donors. On-going efforts in our laboratory involve accessing reduced oxidation states of **1** for more thorough electronic structure measurements and chemical reactivity studies.

Start-up funds to N.P.M. were provided by the UIC Department of Chemistry. EPR facilities are supported by the National Biomedical EPR Center Grant EB001980 from NIH. The authors are grateful to members of the Mankad group for verifying reproducibility of the synthetic procedures.

## Notes and references

- 1 S. R. Pauleta, S. Dell'Acqua and I. Moura, *Coord. Chem. Rev.*, 2013, **257**, 332–349.
- 2 K. Brown, M. Tegoni, M. Prudêncio, A. S. Pereira, S. Besson, J. J. Moura, I. Moura and C. Cambillau, *Nat. Struct. Biol.*, 2000, **7**, 191–195.
- 3 T. Rasmussen, B. C. Berks, J. Sanders-Loehr, D. M. Dooley, W. G. Zumft and A. J. Thomson, *Biochemistry*, 2000, **39**, 12753–12756.
- 4 A. Pomowski, W. G. Zumft, P. M. H. Kroneck and O. Einsle, *Nature*, 2011, **477**, 234–237.
- 5 E. M. Johnston, S. Dell'Acqua, S. Ramos, S. R. Pauleta, I. Moura and E. I. Solomon, *J. Am. Chem. Soc.*, 2013, **136**, 614–617.
- 6 R. Sarangi, J. T. York, M. E. Helton, K. Fujisawa, K. D. Karlin, W. B. Tolman, K. O. Hodgson, B. Hedman and E. I. Solomon, *J. Am. Chem. Soc.*, 2008, **130**, 676–686.
- 7 E. C. Brown, J. T. York, W. E. Antholine, E. Ruiz, S. Alvarez and W. B. Tolman, *J. Am. Chem. Soc.*, 2005, **127**, 13752–13753.
- 8 I. Bar-Nahum, A. K. Gupta, S. M. Huber, M. Z. Ertem, C. J. Cramer and W. B. Tolman, *J. Am. Chem. Soc.*, 2009, **131**, 2812–2814.
- 9 R. Sarangi, L. Yang, S. G. Winikoff, L. Gagliardi, C. J. Cramer, W. B. Tolman and E. I. Solomon, *J. Am. Chem. Soc.*, 2011, **133**, 17180–17191.
- 10 J. F. Berry, *Chem. – Eur. J.*, 2010, **16**, 2719–2724.
- 11 S. Alvarez, R. Hoffmann and C. Mealli, *Chem. – Eur. J.*, 2009, **15**, 8358–8373.
- 12 V. W.-W. Yam, W.-K. Lee and T.-F. Lai, *J. Chem. Soc., Chem. Commun.*, 1993, 1571.
- 13 B. J. Johnson, S. V. Lindeman and N. P. Mankad, *Inorg. Chem.*, 2014, **53**, 10611–10619.
- 14 J. T. York, I. Bar-Nahum and W. B. Tolman, *Inorg. Chim. Acta*, 2008, **361**, 885–893.
- 15 G. N. Di Francesco, A. Gaillard, I. Ghiviriga, K. A. Abboud and L. J. Murray, *Inorg. Chem.*, 2014, **53**, 4647–4654.
- 16 A. C. Lane, M. V. Vollmer, C. H. Laber, D. Y. Melgarejo, G. M. Chiarella, J. P. Fackler Jr, X. Yang, G. A. Baker and J. R. Walensky, *Inorg. Chem.*, 2014, **53**, 11357–11366.
- 17 L. Yang, D. R. Powell and R. P. Houser, *Dalton Trans.*, 2007, 955.
- 18 X. Xie, S. I. Gorelsky, R. Sarangi, D. K. Garner, H. J. Hwang, K. O. Hodgson, B. Hedman, Y. Lu and E. I. Solomon, *J. Am. Chem. Soc.*, 2008, **130**, 5194–5205.
- 19 L. Li, N. N. Murthy, J. Telser, L. N. Zakharov, G. P. A. Yap, A. L. Rheingold, K. D. Karlin and S. E. Rokita, *Inorg. Chem.*, 2006, **45**, 7144–7159.
- 20 M. A. Culpepper, G. E. Cutsail III, B. M. Hoffman and A. C. Rosenzweig, *J. Am. Chem. Soc.*, 2012, **134**, 7640–7643.
- 21 S. M. Smith, S. Rawat, J. Telser, B. M. Hoffman, T. L. Stemmler and A. C. Rosenzweig, *Biochemistry*, 2011, **50**, 10231–10240.
- 22 X. Jiang, J. C. Bollinger, M.-H. Baik and D. Lee, *Chem. Commun.*, 2005, 1043.